Pandey, V. N., & Modak, M. J. (1988) *J. Biol. Chem. 263*, 6068–6072.
Pandey, V. N., Stone, K. L., Williams, K. R., & Modak, M. J. (1987) *Biochemistry 26*, 7744–7748.
Srivastava, A., & Modak, M. J. (1980) *J. Biol. Chem. 255*, 917–921.
Stone, K. L., & Williams, K. R. (1986) *J. Chromatogr. 359*, 203–212.

Kinetic Mechanism Whereby DNA Polymerase I (Klenow) Replicates DNA with High Fidelity†

Robert D. Kuchta, Patricia Benkovic, and Stephen J. Benkovic*
Department of Chemistry, 152 Davey Laboratory, The Pennsylvania State University, University Park, Pennsylvania 16802
Received December 30, 1987; Revised Manuscript Received April 19, 1988

ABSTRACT: A complete kinetic scheme describing the polymerization of correct and incorrect dNTPs by the Klenow fragment (KF) of DNA polymerase I has been developed by using short DNA oligomers of defined sequence. The high fidelity arises from a three-stage mechanism. The first stage of discrimination [$(1.1 \times 10^4 \rightarrow 1.2 \times 10^6)$-fold] comes primarily from a dramatically reduced rate of phosphodiester bond formation for incorrect nucleotides, but it also gains a smaller contribution from selective dNTP binding. After phosphodiester bond formation, a conformational change slows dissociation of the incorrect DNA products from KF and, in conjunction with editing by the 3′→5′-exonuclease, increases fidelity 4–>61-fold. Finally, KF polymerizes the next correct dNTP onto a mismatch very slowly, providing a further 6–>340-fold increase in fidelity. Surprisingly, the 3′→5′-exonuclease did not in its hydrolysis reaction differentiate between correctly and incorrectly base-paired nucleotides; rather, an increased lifetime of the enzyme–DNA complex containing the misincorporated base is responsible for discrimination.

DNA polymerase I (pol I)[1] from *Escherichia coli* is a multifunctional enzyme that catalyzes DNA-directed DNA synthesis and is involved in both replication and repair of DNA in vivo (Kornberg, 1980). In addition to catalyzing DNA polymerization, the enzyme also contains a 3′→5′-exonuclease and a 5′→3′-exonuclease. Recently, the complete kinetic scheme of the polymerization reaction was determined (Kuchta et al., 1987).

A critical feature of pol I is the extremely high fidelity with which it synthesizes DNA. The error frequency may be as low as 10^{-8}–10^{-12} errors per nucleotide polymerized (Englisch et al., 1985). This is much less than the error frequency of 0.2–0.0006 errors per nucleotide polymerized predicted on the basis of energy differences between correct and incorrect base pairs (Loeb & Kunkel, 1982).

The kinetic mechanism by which pol I achieves high fidelity remains obscure, although many models have been proposed (Bernardi et al., 1979; Brutlag & Kornberg, 1972; Clayton et al., 1979; Hopfield, 1974, 1980; Ninio, 1975). In each of these models pol I selects for the correct dNTP during two distinct and separate processes, thereby obtaining increased fidelity. These processes have typically been ascribed to the selection of the correct dNTP (El-Deiry et al., 1984; Fersht et al., 1982) and the removal of misincorporated nucleotides by the 3′→5′-exonuclease (Brutlag & Kornberg, 1972; Kunkel et al., 1981a). More recently, a rate-determining conformational change prior to phosphodiester bond formation has been implicated (Ferrin & Mildvan, 1986; Mizrahi et al., 1985).

In the present study, the kinetic parameters governing misincorporation, polymerization onto a mismatched 3′ terminus, and removal of mismatches by the 3′→5′-exonuclease were measured by using short DNA oligomers of defined sequence. We then constructed a scheme that reveals how fidelity results from amplification of the discrimination occurring in three distinct kinetic steps.

Chart I: DNA Duplexes

9/20-mer[a]	TCGCAGCCG(3′) AGCGTCGGCAGGTTCCCAAA	9A/20-mer[b]	TCGCAGCCGA(3′) AGCGTCGGCAGGTTCCCAAA
13/20-mer	TCGCAGCCGTCCA(3′) AGCGTCGGCAGGTTCCCAAA	9C/20-mer	TCGCAGCCGC(3′) AGCGTCGGCAGGTTCCCAAA
16/19-mer	TGCGTCCGGCGTAGAG(3′) CGCAGGCCGCATCTCCTAG	13T/20-mer	TCGCAGCCGTCCAT(3′) AGCGTCGGCAGGTTCCCAAA
9/36-mer	GCCTCGCAG(3′) CGGAGCGTCGGCAGGTTGGTTGAGTAGGTCTTGTTT		
12/36-mer	GCCTCGCAGCCG(3′) CGGAGCGTCGGCAGGTTGGTTGAGTAGGTCTTGTTT		

[a] The labels denote the length of the primer/template. Those duplexes consisting of only two numbers (e.g., 9/20-mer) are correctly base-paired. The template base(s) to be copied along with the 3′-terminal base(s) of the primer/template is (are) included in the text after each DNA [e.g., 9/20-mer ($^{CG}_{GCAGG}$)]. [b] The labels containing a letter have a mismatched primer 3′-terminus. For example, the 9A/20-mer is the 9/20-mer with an A appended to the primer 3′-terminus and which forms an A–A base pair.

Experimental Procedures

Materials. New England Nuclear supplied (S_P)-[^{35}S]-dATPαS, [^{32}P]PP_i and [^{32}P]dNTPs. Pharmacia provided

† This work was supported by NIH Grant GM13306 (S.J.B.) and NIH Postdoctoral Fellowship GM11309 (R.D.K.).
* Address correspondence to this author.

[1] Abbreviations: EDTA, ethylenediaminetetraacetate, sodium salt; KF, Klenow fragment of DNA polymerase I; pol I, DNA polymerase I; PP_i, sodium pyrophosphate; Tris·HCl, tris(hydroxymethyl)aminomethane, hydrochloride salt.

0006-2960/88/0427-6716$01.50/0

Chart II: Assays for Error Accumulation

DNA used	misincorporation of				at template position and base
	dATP	dCTP	dGTP	dTTP	
9/20-mer	20 μM dATP	20 μM dCTP	20 μM dGTP	–	10, A
9/20-mer	20 μM dATP 1 μM dTTP	–	20 μM dGTP 1 μM dTTP	20 μM dTTP	11, G
9/20-mer	–	–	–	–	12, G
9/20-mer	–	20 μM dCTP 1 μM dTTP	20 μM dGTP 1 μM dTTP 1 μM dCTP	20 μM dTTP 1 μM dCTP	13, T
13/20-mer	–	20 μM dCTP	20 μM dGTP	20 μM dTTP	14, T
13/20-mer	20 μM dATP	20 μM dCTP 1 μM dATP	–	20 μM dTTP 1 μM dATP	15, C

unlabeled dNTPs. PP_i was purified and quantitated as described previously (Kuchta et al., 1987). KF was purified from *E. coli* CJ155 (Joyce & Grindley, 1983) and quantitated spectrally by using $\epsilon_{278} = 6.32 \times 10^4$ M^{-1} cm^{-1} (Setlow et al., 1972). Dr. C. Joyce kindly provided the bacterial strain CJ155, and Dr. Jin-Tann Chen kindly provided (S_P)-dATPαS.

DNA. DNA oligomers were synthesized by using an Applied Biosystems 380A DNA synthesizer. DNA duplex formation was performed according to the method of Kuchta et al. (1987), except the reactions were heated to 70 °C for 5 min rather than boiled. The concentration of DNA duplexes (Chart I) was determined essentially as before (Kuchta et al., 1987). For the mismatch containing duplexes 9A/20-mer, 9C/20-mer, and 13T/20-mer, the concentrations were measured in the same manner as that of 9/20-mer or 13/20-mer except [^{32}P]dNMP incorporation into DNA was measured after 5–45 min rather than 15 s–2 min. 3′-[^{3}H]dA-labeled 14/20-mer was synthesized as previously described (Kuchta et al., 1987).

Incorporation of radioactivity into DNA was measured by a DE81 (Whatman) filter binding assay (Bryant et al., 1983) and scintillation counting. We used Fisher Scintiverse II cocktail and either a Beckman LS8100 or LS6800 scintillation counter.

5′-^{32}P-End Labeling of DNA. DNA oligomers were 5′-^{32}P-end labeled by using cloned polynucleotide kinase (U.S. Biochemical Corp.) and [γ-^{32}P]ATP (Mizrahi et al., 1986).

Data Analysis and Computer Simulation. Computer simulations were performed by using the program Simul (Barshop et al., 1983) that was modified to allow input of data as *x*,*y* pairs (Anderson et al., 1987). The data for dATP misincorporation into 9/20-mer were initially fit to the model in Scheme V by trial and error. Directly measured rate constants [k_{exo}, k_{off} (9A/20-mer), K_D (9/20-mer), and K_D (dATP) (B. Eger, unpublished data)] were held constant. Additionally, the rate of k_{exo} was limited by the pre-steady-state burst data. The dATP concentration dependence of the data requires $K_3 \leq 1$.

Electrophoresis. DNA oligomers were separated by electrophoresis on denaturing 10–14% acrylamide gels, and ^{32}P-labeled DNA was visualized by autoradiography (Mizrahi et al., 1986). The amount in various bands was quantitated by their excision from the gel and scintillation counting in 3 mL of Fisher Scintiverse II cocktail.

Enzyme Assays. Unless noted, all assays contained 5 mM $MgCl_2$ and 50 mM Tris·HCl, pH 7.4 at room temperature.

Accumulation of Errors. Qualitative examination of errors that accumulate used assays that contained 130 nM 9/20-mer or 13/20-mer and 250 nM KF in standard assay buffer. The DNA and the dNTP mixtures used were those listed in Chart II with the 20 μM dNTPs replaced with 11.2 μM [α-^{32}P]-dNTPs (approximately 40000 cpm $pmol^{-1}$). Incorrect products were detected by gel electrophoresis.

Assays to measure the accumulation rates of various errors contained 100 nM 5′-^{32}P-labeled DNA and 50 nM KF in standard assay buffer. Aliquots were withdrawn between 0 and 30 min and quenched into gel loading buffer. The amount of incorrect product was quantitated by gel electrophoresis. Chart II lists the DNA and dNTP mixtures used to scan for errors at each position.

Measurement of dNTP → dNMP. Formation of dNMP from dNTP was measured by incubating 50 nM KF, 100 nM DNA, and 5 μM [α-^{32}P]dNTP (approximately 10000 cpm $pmol^{-1}$) in standard assay buffer. Aliquots were withdrawn at various times (0–60 min) and quenched with EDTA to a final concentration of 20–40 mM. The samples were spotted on PEI–cellulose TLC plates with indicator (Baker) along with 6 nmol of dNTP and dNMP as markers. The plates were developed with 0.3 M sodium phosphate, pH 7. After the dNTP and dNMP were located via fluorescence and autoradiography, the amount of [^{32}P]dNMP was determined by cutting the plate into sections followed by scintillation counting in 3 mL of scintillation fluid.

Formation of [^{32}P]dNTP from [^{32}P]PP_i and dNMP. Reactions contained 2 mM dithiothreitol, 6 mM $MgCl_2$, 1 mM [^{32}P]PP_i (1000 cpm $pmol^{-1}$), and 50 nM KF along with either 33 nM poly(dA), 600 nM oligo(dT_{10}), 100 μM dTTP, and 1 mM dGMP or 33 nM poly(dC), 600 nM oligo(dG_{12-18}), 100 μM dGTP, and 1 mM dAMP. After 0–90 min, 3-μL aliquots were mixed with 0.4 unit of yeast inorganic pyrophosphatase (Sigma) and allowed to react for 1 min, at which time EDTA was added to quench the reaction. This converted all of the PP_i to orthophosphate. The amount of [^{32}P]dNTP was quantitated by TLC on PEI–cellulose plates as above.

Reactions to measure exchange of [^{32}P]PP_i into dATP with the 12/36-mer and 9/20-mer contained 1 μM DNA, 20 μM dATP, 0.5 μM KF, and 100 μM [^{32}P]PP_i. After 0–30 min, aliquots were quenched by the addition of EDTA, and the amount of [^{32}P]dATP was determined by TLC as above.

Kinetics of Misincorporation. Misincorporation of dGTP into 16/19-mer was measured by incubating 70 nM 16/19-mer, 25 nM KF, and 7–42 μM [α-^{32}P]dGTP (approximately 5000 cpm $pmol^{-1}$) in standard assay buffer. Aliquots were quenched with EDTA at various times, and the amount of [^{32}P]dGMP incorporated into DNA was quantitated with the DE81 filter binding assay.

Misincorporation of dATP into 9/20-mer and 12/36-mer was measured in assays containing 1.62 μM DNA, 16 nM KF, and 5.2–21 μM [α-^{32}P]dATP (approximately 50000 cpm $pmol^{-1}$) in standard assay buffer. At various times aliquots were quenched into gel loading buffer containing 80% formamide. 3′-[^{32}P]dA-labeled 9A-mer or 12A-mer was quantitated by gel electrophoresis and scintillation counting.

Pre-steady-state misincorporation reactions (30 μL) contained 100 nM 9/36-mer or 12/36-mer, 330 nM KF, 5 μM dGTP, 5 μM dCTP, and 20 μM [α-^{32}P]dATP (400000 cpm

pmol^{-1}). After 10–900 s, aliquots were quenched into gel loading buffer, and the amount of 3′-[^{32}P]dA-labeled 9A-mer or 12A-mer was measured by gel electrophoresis. Alternatively, the DNA was 5′-^{32}P-labeled and nonradioactive dATP was used. Assays to measure pre-steady-state misincorporation into 9/20-mer contained 100 nM 5′-^{32}P-labeled 9/20-mer, 7.5–30 μM dATP, and 330 nM KF and were performed identically with those above.

Measurement of 3′→5′-Exonuclease Rates. (a) Method I in Scheme II. The rate of the 3′→5′-exonuclease (k_{exo}) upon 14/20-mer was measured with assays initiated by adding 125 nM KF to 42 nM 3′-[^{3}H]dA-labeled 14/20-mer in standard assay buffer. The amount of ^{3}H remaining in the DNA at various times was measured with the filter binding assay.

Assays to measure k_{exo} by gel electrophoresis typically contained 50–100 nM 5′-^{32}P-labeled DNA$_n$ in standard assay buffer, and the addition of 200–400 nM KF initiated the assay. Time points were quenched into gel loading buffer, and the amount of substrate (DNA$_n$) and product (DNA$_{n-1}$) was quantitated. The effects of PP$_i$ (0–400 μM) on k_{exo} were measured by this method.

(b) Method II in Scheme II. Assays to measure k_{exo} of 9/20-mer by [^{32}P]dGMP incorporation consisted of 50–200 nM 9/20-mer and 0.5 μM [α-^{32}P]dGTP in standard assay buffer and were started by the addition of 10 nM KF. The amount of [^{32}P]dGMP incorporated into 9/20-mer was quantitated by using the filter binding assay. With 13T/20-mer, k_{exo} was identically obtained except the assay contained 50–200 nM 13T/20-mer, 0.5 μM [α-^{32}P]dATP, 0.5 μM dTTP, and 0.5 μM dGTP. For 9A/20-mer and 9C/20-mer the same methods were used except the assay contained 0.5 μM [α-^{32}P]dCTP, 0.5 μM dATP, 0.5 μM dGTP, 0.5 μM dTTP, and 50–200 nM 9A/20-mer or 9C/20-mer. To measure the effects of high levels of dTTP and dCTP, we used identical protocols. For those assays that contained high concentrations of dCTP, [α-^{32}P]dATP incorporation was monitored and dCTP did not contain ^{32}P.

Measurement of k_{off} for Mismatch Containing DNAs. Equal volumes (45 μL) of KF·DNA (50 nM KF, 50 mM Tris·HCl, pH 7.4, 2 mM EDTA, and 215 nM 9A/20-mer or 9C/20-mer) and 13/20-mer (388 nM 13/20-mer, 10 μM [α-^{32}P]dATP, 50 mM Tris·HCl, pH 7.4, and 12 mM $MgCl_2$) were mixed at 22 °C and then quenched with 142 μL of 0.1 M EDTA, pH 7.4. The amount of [^{32}P]dATP incorporated into 13/20-mer was determined with the filter binding assay. The rate of [^{32}P]dATP incorporation in the absence of 9A/20-mer and 9C/20-mer was determined identically.

Specificity of KF·9/20-mer Generated by Exonuclease Activity. Assays contained 0.87 μM 9A/20-mer or 9/20-mer, 1.7 μM dGTP, and 30.2 μM [α-^{32}P]dATP in standard assay buffer and were initiated by adding 87 nM KF. Time points were quenched into gel loading buffer, and the amount of 3′-[^{32}P]dA-labeled 9A/20-mer was quantitated by gel electrophoresis.

Addition of the Next Correct dNTP to a Mismatch. Assays to measure the rate of polymerization onto the 13T/20-mer contained 5 nM KF, 96 nM 13T/20-mer, 0.5 μM [α-^{32}P]-dTTP, and 55–220 μM dGTP. The rate of [^{32}P]dTMP incorporation into DNA was determined with the filter binding assay after aliquots were quenched at various times with EDTA. Polymerization onto the 9C/20-mer was measured in assays containing 5 nM KF, 120 nM 9C/20-mer, 0.5 μM [α-^{32}P]dATP, 0.5 μM dGTP, and 20–200 μM dCTP. The rate of [^{32}P]dAMP incorporation was determined as described above. Polymerization onto the 9A/20-mer was measured identically with polymerization onto the 9C/20-mer, except 110 nM 9A/20-mer replaced the 9C/20-mer.

Pyrophosphorolysis. 5′-^{32}P-Labeled 9A/20-mer (86 nM) was mixed with 330 nM KF, 140 μM PP$_i$, and 4 μM dATP in standard assay buffer. At various times (0–75 s) samples were quenched into gel loading buffer. The amount of 9A/20-mer and 9/20-mer was quantitated by gel electrophoresis and scintillation counting.

Table I: Rate of Stable Misincorporation into DNA[a]

template position	base	rate of stable misincorporation (s^{-1})			
		dATP	dCTP	dGTP	dTTP
10	A	1.1×10^{-3}	$<2 \times 10^{-5}$	$<3 \times 10^{-5}$	C
11	G	6×10^{-5}	C	9×10^{-4}	4×10^{-4}
12	G	—	C	—	—
13	T	C	2×10^{-4}	$<5 \times 10^{-6}$	4.4×10^{-4}
14	T	C	$<6 \times 10^{-6}$	$<6 \times 10^{-6}$	$<7 \times 10^{-6}$
15	C	$<1 \times 10^{-5}$	$<2 \times 10^{-5}$	C	$<7 \times 10^{-6}$
18[b]	T	C	—	5.9×10^{-3}	—

[a] Rates of misincorporation of each dNTP into the 9/20-mer at various template positions were measured as described under Experimental Procedures. Rates are calculated for pmol of product s^{-1} (pmol of KF)$^{-1}$. "C" indicates the correct dNTP at each template position, and "—" indicates the value was not measured. The rates shown were corrected for misincorporation of other dNTPs (if any) in the reactions. [b] The DNA used for this experiment was the 16/19-mer.

Table II: Kinetic Parameters of Misincorporation

	k_{cat} (s^{-1})	K_M (μM)	k_{cat}/K_M (M^{-1} s^{-1})
(1)[a] 9/20-mer + dATP	0.0021	8.3	2.5×10^2
(2)[a] 12/36-mer + dATP	0.0039	21	1.9×10^2
(3)[a] 17/19-mer + dGTP	0.010	17	5.9×10^2
(4)[b] 13/20-mer + dATP	50	5	1×10^7

[a] The products of each reaction were (1) $\cdots\overset{G}{\underset{G}{}}\overset{A}{\underset{CAG}{}}\cdots$, (2) $\cdots\overset{G}{\underset{CTAG}{}}\overset{A}{\underset{CAG}{}}\cdots$, (3) $\cdots\overset{CAA}{\underset{GTT}{}}\cdots$, and [b] (4) [a correct polymerization (Kuchta et al., 1987)].

RESULTS

Steady-State Misincorporation. Incubation of dGTP with 16/19-mer (Chart I) and KF resulted in rapid dGTP incorporation to form the correct product, 17/19-mer ($^{GG}_{CCTAG}$), but then significant incorporation of a second, incorrect dGTP opposite a template thymidine to form 17G/19-mer ($^{GGG}_{CCTAG}$) followed (Mizrahi et al., 1986). This prompted us to examine other synthetic oligomers for misincorporation (Table I). Misincorporation at various positions along the template was detected by labeling the DNA at the 5′-terminus with ^{32}P and looking for DNA products of incorrect length as well as by incubating unlabeled DNA with [α-^{32}P]dNTPs and examining the DNA products for ^{32}P incorporation by gel electrophoresis. Misincorporation of dATP into the 9/20-mer ($^{CG}_{GCAG}$) is shown in Figure 1. The reported rates were measured at an arbitrary value of 20 μM dNTP. Owing to experimental uncertainty, rates of misincorporation less than 5×10^{-5} s^{-1} are upper limits. Significant misincorporation occurred at several template positions, and the rate and type of misincorporation varied substantially.

The fact that misincorporation occurred at a significant rate allowed us to measure in depth steady-state kinetic parameters for three misincorporations (Table II). In each case there was relatively little discrimination in the K_Ms. Replacing dATP with dATPαS resulted in an elemental effect on misincorporation into 9/20-mer of 5–8 as the dATPαS concentration varied between 48 and 11 μM, indicating that phosphodiester bond formation may be partially rate-limiting during steady-state misincorporation.

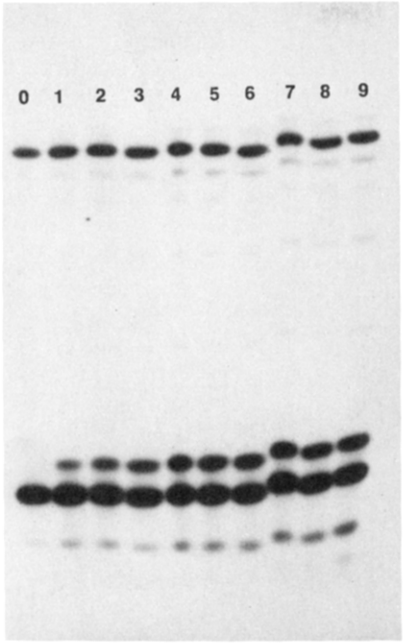

FIGURE 1: Misincorporation of dATP into the 9/20-mer ($^{CG}_{GCAG}$) to form 9A/20-mer ($^{CGA}_{GCAG}$). The reaction contained 0.87 μM 5'-^{32}P-labeled 9/20-mer, 0.3 μM KF, 31 μM dATP, 3 μM dGTP, and 5 mM $MgCl_2$, in 50 mM Tris, pH 7.4. After 2.5, 5, 10, 12.5, 15, 20, 30, 45, and 60 min, 2.5-μL aliquots were quenched into 7.5 μL of gel loading buffer and subjected to gel electrophoresis and autoradiography (lanes 1–9). Lane 0 is the 9/20-mer alone.

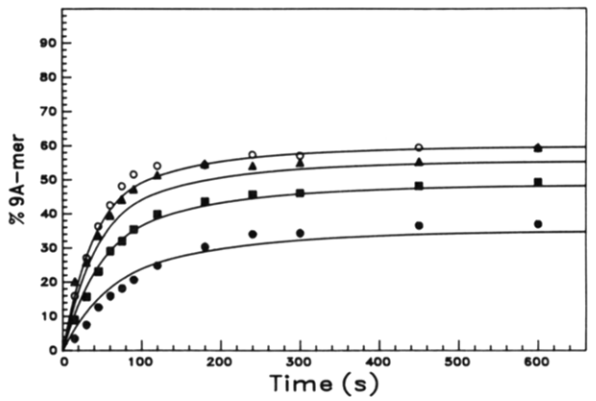

FIGURE 2: Pre-steady-state misincorporation into 9/20-mer. Assays were performed as described under Experimental Procedures and contained 7.5 μM (●), 15 μM (■), 22.5 μM (▲), and 30 μM dATP (○). The lines were generated by computer simulation using the model in Scheme V and the rate constants in Table VI.

Pre-Steady-State Misincorporation. During steady-state misincorporation of dATP into the 9/20-mer ($^{CG}_{GCAG}$) and the 12/36-mer ($^{CG}_{GCAG}$), a small but reproducible "burst" occurred before the first time point at 2.5 min (data not shown). We therefore examined pre-steady-state misincorporation into 9/20-mer under conditions of excess KF (Figure 2). Increasing the dATP concentration increased both the magnitude and the rate of the rapid phase. Replacing dATP (20 μM) with dATPαS resulted in an observed elemental effect of 65 (Figure 3). With 9/20-mer and dCTP, a reaction that does not yield stable misincorporation products, there was no pre-steady-state burst of misincorporation nor slow accumulation of the misincorporation products at these high levels of KF. However, dCMP was produced.

The energy relay model (Hopfield, 1980) posits that KF becomes more accurate after the initial polymerization cycle. To test this hypothesis, we measured the pre-steady-state rate of dATP misincorporation at position 13 of the 12/36-mer

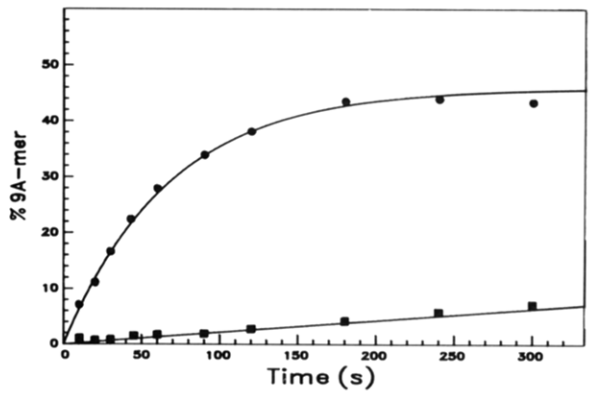

FIGURE 3: Elemental effect on pre-steady-state misincorporation of dATP into the 9/20-mer ($^{CG}_{GCAG}$). Conditions were identical with those in Figure 2 except the assays contained either 20.8 μM dATP (●) or dATPαS (■). With dATP, the rate was determined by fitting the data to an exponential, and with dATPαS the rate was determined directly from the line.

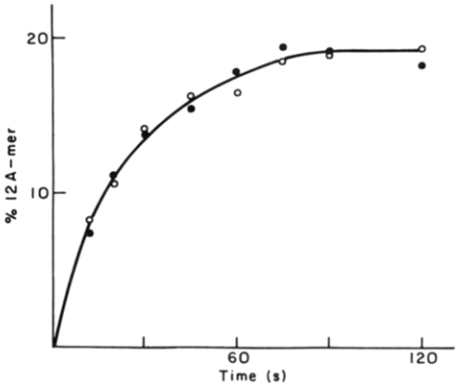

FIGURE 4: Misincorporation before and after three polymerization cycles. The rate of misincorporation of dATP opposite a template A (position 13) in the (○) 9/36-mer ($^{G}_{CGGCAG}$) and (●) 12/36-mer ($^{GCCG}_{CGGCAG}$) to form 12A-mer was measured under conditions of excess KF as described under Experimental Procedures.

Table III: Rates of dNTP → dNMP (s^{-1}) with 5 μM dNTP[a]

DNA	dATP	dCTP	dGTP	dTTP
9/20-mer	13×10^{-4}	13×10^{-4}	3×10^{-4}	8×10^{-4} [b]
13/20-mer	34×10^{-4} [b]	12×10^{-4}	17×10^{-4}	$<2 \times 10^{-5}$

[a] Rates were calculated for pmol of dNMP s^{-1} (pmol of KF)$^{-1}$. [b] Correct nucleotides.

($^{GCCG}_{CGGCAG}$) and 9/36-mer ($^{G}_{CGGCAG}$). The 9/36-mer must undergo three polymerization cycles in order to form 12/36-mer that then can misincorporate dATP. The misincorporation rates for both oligomers were identical [$(46 \pm 7) \times 10^{-3}$ s^{-1}, Figure 4], contrary to the predictions of the energy relay model.[2]

Kinetic Properties of the 3'→5'-Exonuclease. Conversion of dNTPs to dNMPs occurs via incorporation into DNA and then excision of the dNMP by the 3'→5'-exonuclease (Scheme I), thereby providing lower limits of both the polymerase (k_{pol}) and 3'→5'-exonuclease (k_{exo}) rates (Fersht et al., 1983). Table III shows the rate of dNTP → dNMP with the 9/20-mer ($^{CG}_{GCAG}$) and 13/20-mer ($^{CA}_{GTTC}$). For 9/20-mer + dTTP and 13/20-mer + dATP, where the initial polymerization would be a correct incorporation, the dNMP produced most likely arises from idling at the terminus of the 10/20-mer and 14/20-mer, respectively, via pathway II and with the rate

[2] We cannot rule out the possibility that the high accuracy state has a short lifetime. The minimum rate of decay consistent with the data would be 0.3 s^{-1}.

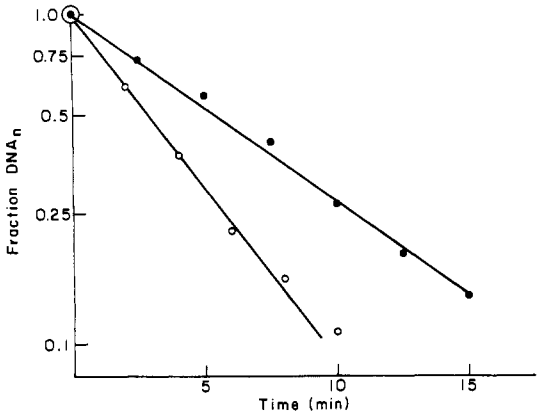

FIGURE 5: Logarithmic plot of the fraction of DNA_n remaining versus time to determine k_{exo}. The rate of the 3′→5′-exonuclease ($DNA_n \rightarrow DNA_{n-1}$) was measured under conditions of excess KF (method I, Scheme II) for the 14/20-mer (●, $^{AA}_{TTCC}$) and 9C/20-mer (○, $^{GC}_{CAGG}$) as described under Experimental Procedures with $k_{exo} = 2 \times 10^{-3}$ s^{-1} and 4.2×10^{-3} s^{-1}, respectively.

mediated by k_{pol} and k_{exo} (Mizrahi et al., 1986). For the 9/20-mer + dGTP, dNMP formation probably proceeds via the 9/20-mer and pathway II, the idling turnover of the terminal base of the 9/20-mer (Mizrahi et al., 1986). For the others dNMP formation occurs solely by pathway I and is also dependent upon k_{pol} and k_{exo}. Further examination of the dATP → dAMP turnover in the presence of the 9/20-mer by varying dATP levels gave $k_{cat} = 5.6 \times 10^{-3}$ s^{-1} and K_M (dATP) = 16 μM. This K_M is very similar to that measured for dATP misincorporation into the 9/20-mer.

Scheme I

$$\text{(I) } DNA_n \xrightarrow[dNTP^*]{k_{pol}} DNA_{n+1} \xrightarrow{k_{exo}} DNA_n + dNMP^*$$

$$\text{(II) } DNA_n \xrightarrow{k_{exo}} DNA_{n-1} \xrightarrow[dNTP^*]{k_{pol}} DNA_n^* \xrightarrow{k_{exo}} DNA_{n-1} + dNMP^*$$

In light of the fact that some misincorporation products accumulate to high levels, we used the methods outlined in Scheme II to explicitly measure k_{exo}. Several precautions were observed to ensure accurate measurements. In method I, the reactions included a large excess of KF so that the rates were pseudo first order. In order to prevent inhibition of the 3′→5′-exonuclease by the DNA products (method II), the reaction contained a large excess of substrate DNA over KF, and the product DNA was converted to the blunt-ended species for which KF has lower affinity. For example, the 9A/20-mer ($^{GA}_{CAGG}$) would be converted to the 9/20-mer ($^{G}_{CAGG}$) and then blunt-ended in the presence of [α-^{32}P]dCTP, dATP, dTTP, and dGTP. Method II measures k_{exo} since $k_{pol} \gg k_{exo}$, and as we will demonstrate later the rate of addition of the next correct dNTP onto a mismatch is much less than k_{exo} under the experimental conditions.

Scheme II

$$\text{(I) } DNA_n \xrightarrow{k_{exo}} DNA_{n-1} \qquad \text{quantitate } DNA_{n-1}$$

$$\text{(II) } DNA_n \xrightarrow{k_{exo}} DNA_{n-1} \xrightarrow{dNTP^*} DNA_n^*$$

quantitate dNTP* incorporation

When tested, both methods yielded identical results (9/20-mer and 9C/20-mer). Measurement of k_{exo} for the 14/20-mer ($^{AA}_{TTCC}$) and 9C/20-mer ($^{GC}_{CAGG}$) using method I is depicted in Figure 5. Method I was used to provide a measure only of k_{exo} and when it was experimentally impossible to use method II [13/20-mer ($^{CA}_{GTTC}$)]. Table IV gives k_{exo} for DNAs with correctly and incorrectly base-paired 3′ termini. Both k_{exo} at saturating DNA and the K_M for DNA varied less than 13-fold. [We assume the K_M for the 13T/20-mer, which was too low to measure in the exonuclease reaction, is equal to the K_D of 5 nM for the 9/20-mer and 13/20-mer measured from the polymerization reaction (Kuchta et al., 1987).] Comparison of the specificity parameter k_{exo}/K_M reveals only very slight differences among the DNAs.

Table IV: 3′→5′-Exonuclease Rates with Various DNAs[a]

DNA	k_{exo} (s^{-1})	K_M (DNA) (nM)	k_{exo}/K_M (M^{-1} s^{-1})
14/20-mer	2×10^{-3}	— (5)	4×10^5
13/20-mer	1.5×10^{-3}	— (5)	3×10^5
9/20-mer	7×10^{-4}	<20 (5)	1.4×10^5
13T/20-mer	3.4×10^{-3}	<20 (5)	6.8×10^5
9C/20-mer	$(4.5 \pm 1.5) \times 10^{-3}$	24	1.9×10^5
9A/20-mer	$(8.2 \pm 1.7) \times 10^{-3}$	64	1.3×10^5

[a] k_{exo} and K_M were measured as described under Experimental Procedures. For the 14/20-mer, 13/20-mer, and 9/20-mer a dAMP, dAMP, or dGMP, respectively, is excised from the 3′ terminus. A dash indicates the value was not measured. For the K_Ms, the 5 nM in parentheses is the measured K_D of 9/20-mer and 13/20-mer (Kuchta et al., 1987) and was used to calculate k_{exo}/K_M values. For the 13/20-mer and 14/20-mer, method I of Scheme II was used, and therefore only k_{exo}s were obtained, while in the other cases method II was used to determine k_{exo} and K_M.

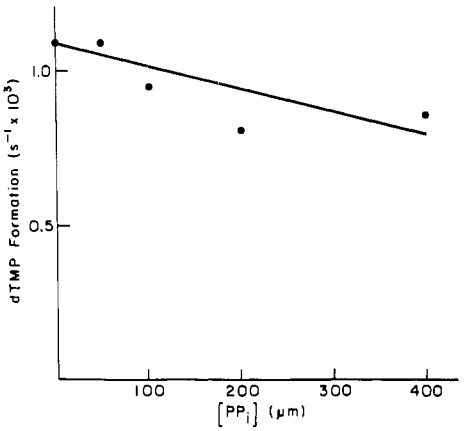

FIGURE 6: Effect of PP_i on dTTP hydrolysis in the presence of the 9/20-mer ($^{CG}_{GCAG}$). dTMP formation from dTTP was determined as described under Experimental Procedures as the concentration of PP_i varied from 0 to 400 μM.

Addition of either dTTP or dCTP up to concentrations of 200 μM inhibited the exonuclease activity of KF less than 20% toward the mismatch at the terminus of the 9A/20-mer ($^{GA}_{CAGG}$). On the other hand, addition of 3.8 μM dGTP (the next correct dNTP) abolished exonuclease activity on 3′-[^{3}H]dA-labeled 14/20-mer ($^{AA}_{TTCC}$), which contains a correctly base-paired terminus. Thus, exogenous dNTPs do not significantly inhibit exonuclease activity but rather prevent excision of a specific base when the added dNTP permits rapid polymerization beyond that site.

The exonuclease clearly functions in the KF·DNA_n complex to form dNMPs. To demonstrate that it also functions within the KF·DNA_n·PP_i complex, we included 50–400 μM PP_i (K_D = 100 μM; Kuchta et al., 1987) in assays for dTMP formation from dTTP and the 9/20-mer ($^{CG}_{GCAG}$), where a correct base is being incorporated and excised (Figure 6). PP_i (400 μM) inhibited dTMP production only 23%, even though 80% of the KF·DNA_n contains bound PP_i. Similarly, for two oligonucleotides containing incorrectly base-paired termini, the presence of 400 μM PP_i did not inhibit the exonuclease. For the 9A/20-mer ($^{GA}_{CAGG}$), an incorrect product that accumulates

Scheme III

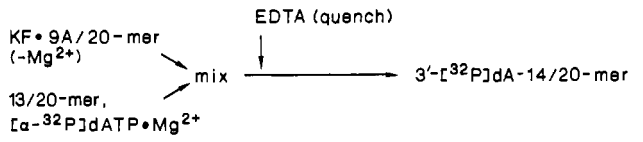

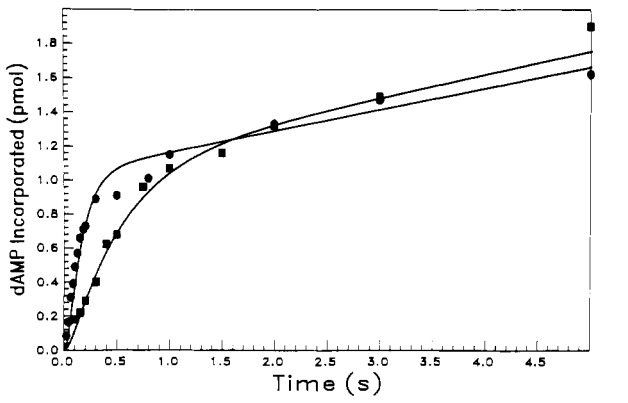

FIGURE 7: Dissociation rates of KF•9A/20-mer ($^{GA}_{CAGG}$). The rate of formation of 3'-[^{32}P]dA-labeled 14/20-mer was measured as described in Scheme III under Experimental Procedures with (■) and without (●) 9A/20-mer (DNA_1). The lines were generated via computer simulation of the model in Scheme IV.

from 9/20-mer + dATP, the rates were 8×10^{-3} s^{-1} (+PP_i) and 11×10^{-3} s^{-1} (–PP_i). With the 9C/20-mer ($^{GC}_{CAGG}$), an incorrect product that does not accumulate from 9/20-mer + dCTP, the rates were 4.3×10^{-3} s^{-1} (+PP_i) and 3.6×10^{-3} s^{-1} (–PP_i).

Since these data were obtained by measuring DNA_{n-1} production (method I, Scheme II) the results also indicate that PP_i does not rapidly excise incorrectly base-paired nucleotides. Whereas pyrophosphorolysis of a correctly base-paired nucleotide exhibited burst kinetics (rapid dNTP formation; Kuchta et al., 1987), in this case pyrophosphorolysis was not rapid. Additionally, experiments that measured [^{32}P]PP_i exchange into dATP during the misincorporation cycle with 12/36-mer ($^{CG}_{GCAG}$) and 9/20-mer ($^{CG}_{GCAG}$) provide further evidence against the involvement of pyrophosphorolysis in mismatch excision. They revealed only a slow rate of [^{32}P]dATP formation, 2×10^{-4} s^{-1} and 5×10^{-5} s^{-1}, respectively, and no rapid initial phase of exchange.

The KF•DNA_n complex generated by exonuclease action on KF•DNA_{n+1} or the admixing of KF and DNA_n discriminates equally against incorrect dNTPs. Incubations of KF and 30 μM [α-^{32}P]dATP with either 9/20-mer ($^{CG}_{GCAG}$) or 9A/20-mer ($^{CGA}_{GCAG}$) formed 3'-[^{32}P]dA-labeled 9A/20-mer with rates of 1.4×10^{-3} s^{-1} (9/20-mer) and 2.5×10^{-4} s^{-1} (9A/20-mer). The slower rate of [^{32}P]dATP incorporation with 9A/20-mer is due to the slow rate of the exonuclease (8×10^{-3} s^{-1}) and relatively rapid rate of KF•9/20-mer dissociation (0.17 s^{-1}; Kuchta et al., 1987). If after excision of the mismatched base the resultant KF•DNA_n complex exhibited lowered specificity, one would expect a greater rate of dATP misincorporation, contrary to the data.

Fate of Incorrect DNA_{n+1}. After polymerization of an incorrect dNTP into DNA_n, one of three fates awaits the KF•DNA_{n+1} complex: (1) removal of the incorrect base via the exonuclease (k_{exo}); (2) dissociation of the DNA_{n+1} (k_{off}); or (3) polymerization of the following correct dNTP onto the mismatch. We measured DNA dissociation by a rapid quench technique as shown in Scheme III, and this yielded the data in Figure 7. Scheme IV accurately describes the data where previous work (Kuchta et al., 1987) elucidated the k_{off}/k_{on} for the 14/20-mer ($^{AA}_{TTCC}$) and k_{pol} = 7.7 s^{-1} for the 13/20-mer

Table V: Rate of Addition of the Next Correct dNTP onto a Mismatch

reaction	k_{cat} (s^{-1})	K_M (dNTP) (μM)	k_{cat}/K_M (M^{-1} s^{-1})
13T/20-mer + dGTP[a]	$<10^{-5}$	—	—
9A/20-mer + dCTP[a]	$<2 \times 10^{-5}$	—	—
9C/20-mer + dCTP	1.4×10^{-2}	75	187
13/20-mer + dATP[b]	50	5	1×10^7

[a] The k_{cat} values for 13T/20-mer and 9A/20-mer were measured at 200 μM dGTP and dCTP, respectively. [b] Incorporation of dATP into 13/20-mer is the addition of dNTP onto a correctly base-paired 3' terminus.

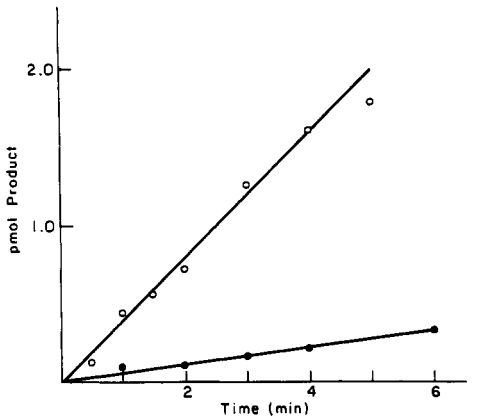

FIGURE 8: Addition of the next correct nucleotide (dCTP) to the 9C/20-mer ($^{GC}_{CAGG}$). Assays were performed as described under Experimental Procedures and contained 200 μM dCTP and either 0.125 μM 9C/20-mer (○, $^{GC}_{CAGG}$) or 9/20-mer (●, $^{G}_{CAGG}$).

($^{A}_{TTCC}$). For the 9A/20-mer ($^{GA}_{CAGG}$), k_{off} = 3.25 s^{-1}, while for 9C/20-mer ($^{GC}_{CAGG}$), k_{off} = 3 s^{-1} (data not shown). For the correct 10/20-mer ($^{GT}_{CAGG}$), k_{off} = 0.17 s^{-1} (Kuchta et al., 1987).

Scheme IV

$$KF{\cdot}DNA_1 \xrightarrow{k_{off}} DNA_1 + KF \xrightarrow[k_{pol}]{13/20\text{-mer, dATP}^*}$$

$$KF{\cdot}14^*/20\text{-mer} \underset{1.2 \times 10^7\ M^{-1}\ s^{-1}}{\overset{0.06\ s^{-1}}{\rightleftharpoons}} KF + 14^*/20\text{-mer}$$

Table V lists the rate of addition of the next correct dNTP onto three mismatches as illustrated for the 9C/20-mer ($^{GC}_{CAGG}$) in Figure 8. That dTTP contamination of the dCTP is not the cause of the observed rate with 9C/20-mer ($^{GC}_{CAGG}$) is supported by the fact that after substitution of 9/20-mer ($^{G}_{CAGG}$) for the 9C/20-mer, the observed rate of dCTP addition actually decreased 6-fold. Gel electrophoresis revealed that reactions containing 9C/20-mer ($^{GC}_{CAGGTTC}$) and [^{32}P]dCTP yielded only 12/20-mer, while inclusion of [^{32}P]dCTP and dATP yielded only 14/20-mer. Thus, while KF polymerized the first dCTP onto the mismatch slowly, it added latter nucleotides rapidly and thereby "locked in" the mismatch.

Discussion

These studies were carried out to elucidate the kinetic mechanisms by which pol I replicates DNA with such remarkable fidelity. They have allowed us to assess the relative contributions of various processes to fidelity and to construct a unified kinetic model (Scheme V and Table VI) that expands upon the minimal kinetic mechanism for correct polymerization (Kuchta et al., 1987) and accurately describes the kinetics of misincorporation. Pol I discriminates so precisely by selecting for the correct nucleotide three times during the cat-

Table VI: Rate and Equilibrium Constants for the Kinetic Mechanism of KF[a]

13/20-mer + dATP[b] (correct)			9/20-mer + dATP[c] (incorrect)	
	5 nM	K_1	5 nM	
	5 μM	K_2	—	
	50 s^{-1}	k_3	—	
k_f = 9.1 × 10^6 M^{-1} s^{-1}	0.5 s^{-1}	k_{-3}	—	k_f = 770 M^{-1} s^{-1}
k_r = 0.18 s^{-1}	1000 s^{-1}	k_4	—	k_r = 0.0033 s^{-1}
	400 s^{-1}	k_{-4}	—	
$k_f \geq$ 50 s^{-1}	>50 s^{-1}	k_5	—	k_f = 0.0035 s^{-1}
$k_r \geq$ 5 × 10^5 M^{-1} s^{-1}	>50 s^{-1}	k_{-5}	—	k_r = 35 M^{-1} s^{-1}
	100 μM	K_6	—	
	0.06 s^{-1}	k_7	3.25 s^{-1}	
	1.2 × 10^7 M^{-1} s^{-1}	k_{-7}	1.2 × 10^7 M^{-1} s^{-1}	
	0.002 s^{-1}	k_{exo}	0.009 s^{-1}	

[a] Rate constants correspond to each step in Scheme V. [b] Rate constants for a correct polymerization are from Kuchta et al. (1987). The values for $k_{\pm 4}$ and $k_{\pm 5}$ are estimates. The forward (k_f) and reverse (k_r) net rate constants for $K_2 \rightarrow k_4$ and $k_5 \rightarrow K_6$ were calculated according to the method of Cleland (1975). [c] The net rate constants for dATP misincorporation into the 9/20-mer were calculated from the following individual rate constants: K_2 = 40 μM, k_3 = 0.035 s^{-1}, k_{-3} = 1.2 s^{-1}, k_4 = 9 s^{-1}, k_{-4} = 0.028 s^{-1}, k_5 = 0.0035 s^{-1}, k_{-5} = 0.0035 s^{-1}, and K_6 = 100 μM. The fit to the data in Figure 1 and Table VIII was determined as described under Experimental Procedures. Although this set of rate constants adequately describes the data (see Figure 1 and Table VIII), it may not be unique.

Scheme V

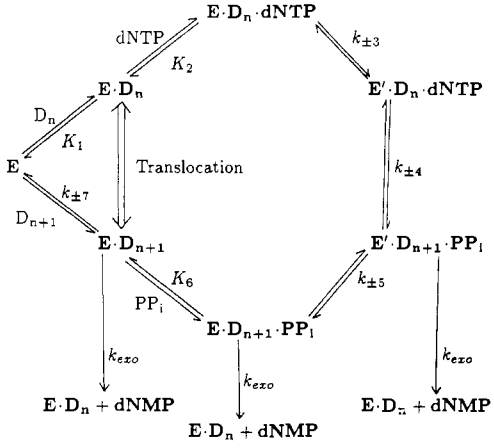

alytic cycle. In the first stage, the high free energy barrier of the chemical step along with discrimination of variable importance during dNTP binding prevents most misincorporation. The second conformational change, k_5, decreases the dissociation rate of mismatch containing DNA, thereby allowing the rather inefficient exonuclease to remove most mismatches. The last stage is the slow rate of addition of the next correct dNTP onto a mismatch, again allowing the exonuclease to remove mismatches. We now describe the evidence for each stage and its contribution to fidelity.

Stage 1. KF initially discriminates against incorrect dNTPs during dNTP binding and later in phosphodiester bond formation in step k_4. We cannot comment on whether the value of k_3 differs for correct and incorrect dNTPs. However, during stable misincorporation of several dNTPs, there was surprisingly little difference between the K_M for correct and incorrect dNTPs (Table II). In light of the rapid dNTP dissociation rate (Bryant et al., 1983) and the slow rate of misincorporation, these data may reflect a lack of discrimination in the dNTP binding step (K_2). Recent data, however, indicate that the amount of selectivity in binding varies 0–100-fold according to the nature of the DNA sequence (B. Eger, unpublished data).

Table VII: Selectivity Obtained by KF at Each Stage[a]

stage 1	1.1 × 10^4->1.2 × 10^6
stage 2	4->60
stage 3	6->340

[a] The values were calculated as described in the text for 5 μM dNTP.

Consequently, much of the initial discrimination occurs during phosphodiester bond formation. We deduce this from the large elemental effect (k^{P-O}/k^{P-S}) of 65 on pre-steady-state misincorporation into 9/20-mer. The actual elemental effect may be smaller than that observed owing to the large elemental effect (≥100; Gupta et al., 1984) on the exonuclease step since the data in Figure 1 represent an approach to equilibrium where the observed rate constant is the sum of contributions from the polymerase and exonuclease activities.

The data allow limits to be placed on the amount of selectivity expressed in stage 1 (Table VII) by comparing the polymerization rates of correct and incorrect dNTPs (Table II) at 5 μM dNTP. For the lower limit we compared the rates of 17/19-mer ($^{GG}_{CCTA}$) + dGTP (2.2 × 10^{-3} s^{-1}) to 13/20-mer ($^{CA}_{GTTC}$) + dATP (25 s^{-1}). To establish the upper limit the maximum estimated rate of dTTP → dTMP with 13/20-mer (<2 × 10^{-5} s^{-1}, Table III) was compared to the same standard. The upper limit represents that situation where the incorrect base is not stably misincorporated. As shown below, the lower limit may be less due to stage 2 discrimination.

Stage 2. The second stage at which KF discriminates against misincorporation is a step with no obvious chemistry designated k_5. Evidence for this step derives from the following observations: (i) The elemental effects for pre-steady-state (65) and steady-state (5–8) misincorporation are dramatically different. (ii) Misincorporation of dATP into the 9/20-mer ($^{CG}_{GCAG}$) displays biphasic kinetics. (iii) In certain cases, i.e., 13/20-mer + dGTP, 13/20-mer + dCTP, and 9/20-mer + dCTP, we observed dNTP turnover (Table III) but no accumulation (Table I) of the expected incorrect products. However, the rates of KF·DNA dissociation for both correct (13/20-mer, 0.06 s^{-1}) and mismatch containing DNA (9C/20-mer ($^{CGC}_{GCAG}$), 3 s^{-1}) are much faster than k_{exo} (1–10 × 10^{-3} s^{-1}). This would seem to predict that all DNA products of incorrect dNTP incorporation should accumulate at approximately the rate of incorporation and that a lag should have occurred in dNMP formation. The data, however, are not consistent with this argument.

We conclude that a nonchemical step, k_5, must be included to provide additional time for excision of the incorrectly incorporated dNTP. That this step precedes PP_i release derives from the observation that the rate of [^{32}P]PP_i exchange into an incorrect dNTP was much slower than the rate of misincorporation, and no "burst" of exchange occurred.[3] An alternative explanation is that the rate constant for PP_i binding decreases to approximately 2 M^{-1} s^{-1}.[4] This is 10^6-fold less

[3] Evidence for PP_i release following k_5 is the lack of [^{32}P]PP_i exchange into dCTP in the presence of KF and 9/20-mer, a case with no stable misincorporation. In order to account for dCTP to dCMP turnover (which requires formation of 9C/20-mer) but no pre-steady-state burst of 9C/20-mer formation, the K_{eq} for phosphodiester bond formation, K_4, must be less than 1. If PP_i release (K_D = 100 μM; Kuchta et al., 1987) precedes k_5, then PP_i exchange should have occurred since the equilibrium is in favor of dNTP formation; however, no exchange was detected.

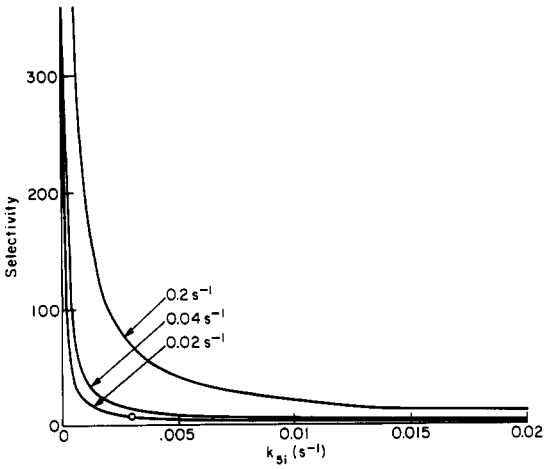

FIGURE 9: Simulation of the effects of varying k_{exo}/k_5 on selectivity. Selectivity (stage 2) was determined as described in the text. k_{exo} was held constant at 0.002, 0.004, and 0.02 s^{-1} and k_{5i} varied. The open circle represents k_{exo} and k_{5i} for KF.

than the rate of diffusion and thus seems unlikely. PP_i release therefore follows k_5, and exogenous PP_i is not involved in stage 2 selectivity.

The amount of selectivity in stage 2 is described in eq 1, where k_i or k^i and k^c or k_c refer to rates for incorrect and correct substrates, respectively. For correct polymerization,

$$\text{selectivity (stage 2)} = \frac{k_{5i} + k^i_{exo}}{k_{5i}} \Big/ \frac{k_{5c} + k^c_{exo}}{k_{5c}} \quad (1)$$

k_5 is kinetically invisible (Kuchta et al., 1987), therefore $k_{5c} \geq 50\ s^{-1}$ and the term $(k_{5c} + k^c_{exo}/k_{5c} = 1$ owing to $k^c_{exo} = 1\text{–}2 \times 10^{-3}\ s^{-1}$. The upper limit for selectivity was estimated from the reaction of 9/20-mer ($^{CG}_{GCAG}$) + dCTP ($k_{5i} \leq 7 \times 10^{-5}\ s^{-1}$ and $k_{exo} \approx 4.5 \times 10^{-3}\ s^{-1}$),[5] where stage 2 increases fidelity ≥60-fold. For the 9/20-mer + dATP, computer simulation of the data indicated that $k_{5i} \approx 3 \times 10^{-3}\ s^{-1}$ and $k_{exo} \approx 9 \times 10^{-3}\ s^{-1}$. Therefore, we find for a lower limit that stage 2 increases fidelity ≤4-fold. Importantly, while k_{5c}/k_{5i} (9/20-mer + dCTP) $\geq 7 \times 10^5$, selectivity is much less (≥60), owing to the slow rate of the exonuclease. Figure 9 shows the relationship between k_{exo}/k_{5i} and stage 2 selectivity, where KF operates at or below the position of the open circle. Clearly the fidelity of KF would be greatly enhanced by a modest increase in k_{exo}.

Stage 3. The final opportunity for KF to increase fidelity is stage 3 or classical proofreading. Our data indicate that under k_{cat} conditions the exonuclease exhibits a small preference toward mismatches (Table III), consistent with previous observations (Brutlag & Kornberg, 1972). However, when the selectivity parameter, k_{cat}/K_M, is considered, there is no discrimination between correctly and incorrectly base-paired DNA. Rather, discrimination during proofreading occurs in the rate of addition of the next correct nucleotide onto a mismatch. The actual amount of selectivity obtained via proofreading is given in eq 2, where k_p and k_{pi} are the rates

$$\text{selectivity (stage 3)} = \frac{k_{pi} + k^i_{exo}}{k_{pi}} \Big/ \frac{k_p + k^c_{exo}}{k_p} \quad (2)$$

of polymerization onto a correct and mismatched 3′ terminus, respectively. Using the values for k_{pi} (Table V) and k_{exo} (Table IV) with 5 μM dNTP, our model predicts that in systems containing only KF proofreading will increase fidelity by 6–>340-fold for the 9C/20-mer ($^{GC}_{CAGG}$) and 13T/20-mer ($^{AT}_{TTCC}$), respectively (Table VII), consistent with previous observations (Fersht, 1979; Fersht et al., 1982; Kunkel et al., 1981a,b, 1986). Further, increasing the concentration of the next correct dNTP does not affect k_{exo} but will increase k_{pi}, thereby accounting for the observed next correct dNTP effects. For the 9C/20-mer, the ratio $k_p/k_{pi} = 28\,000$ with 5 μM dNTP (Table V). In contrast, the actual amount of selectivity, 6, expressed in stage 3 (Table VII) is much less, similar to that of stage 2. This is due to the slow rate of the 3′→5′-exonuclease and raises the intriguing possibility of other cellular 3′→5′-exonucleases with higher rates that would greatly increase fidelity obtained from proofreading.

We considered the possibility that the enzyme form extant after the k_{exo} step might be in a conformation that possessed altered binding and catalytic properties. Experiments designed to misincorporate dATP into KF·9/20-mer ($^{CG}_{GCAGG}$) generated in situ by hydrolysis of the 9A/20-mer ($^{CGA}_{GCAGG}$) exhibited no increased rate of reincorporation of the mismatched dATP.

General Comments. At least three types of mechanisms have been suggested to contribute to the fidelity of base selection by DNA polymerases. These include preferential association of the complementary nucleotide in the initial binding event or selection in a subsequent conformational change prior to phosphodiester bond formation (Fersht et al., 1982; Mizrahi et al., 1985), kinetic proofreading in which the dNTPs are hydrolyzed to dNMP and PP_i before incorporation into the DNA (Hopfield, 1975), and selective hydrolysis of incorporated, mismatched bases by a 3′→5′-exonuclease (Brutlag & Kornberg, 1972). The latter is particularly important for prokaryotic polymerases and may also be important for eukaryotic polymerases (Cotterill et al., 1987).

K_M discrimination has been implicated recently in the case of polymerase α from *Drosophila*, where the ratio of K_M values (incorrect/correct) ranged from 1100 to 2600 for G–T and C–T misincorporations, respectively (Boosalis et al., 1987). Much smaller values have been reported for pol I. Fersht et al. (1983) found that with poly(dA)–oligo(dT), the K_M for incorrect nucleotides increased >100-fold, while El-Deiry et al. (1984, 1988) reported that the K_M for the incorrect nucleotides (dGTP and dATP, respectively) increased only 6–17-fold using poly(dT)–oligo(dA) and poly(dC)–oligo(dG) hook template–primer systems. Our data indicate almost no K_M discrimination for several misincorporations. These apparent discrepancies probably reflect differences in the kinetic profiles of each misincorporation event.

[4] We considered the following model where the slow step after phosphodiester bond formation is PP_i release (k_5):

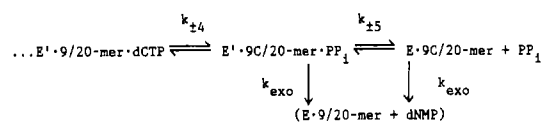

For 9/20-mer + dCTP, $k_5 \leq 7 \times 10^{-5}\ s^{-1}$. Furthermore, to account for the lack of a pre-steady-state burst of misincorporation as well as dCMP formation, $K_4 < 1$ and $k_4 > 1.3 \times 10^{-3}\ s^{-1}$, the rate of dCMP formation in Table III. The rate of excision of the terminal dCMP of the 9C/20-mer via pyrophosphorolysis, k_{PP_i}, is thus described by $k_{PP_i} = (k_{-5} \times [PP_i]k_{-4})/(k_{-4} + k_5)$. This reduces to $k_{PP_i} = k_{-5}[PP_i]$ owing to $k_{-4} \gg k_5$. Since $k_{PP_i} \approx 7 \times 10^{-4}\ s^{-1}$ [the difference between the observed exonuclease rates in the presence and absence of PP_i (see Results)], the rate of PP_i binding, k_{-5}, would have to be only 2 $M^{-1}\ s^{-1}$.

[5] An upper limit of $7 \times 10^{-5}\ s^{-1}$ for k_{5i} was derived from the steady-state rate of 9C/20-mer accumulation ($<2 \times 10^{-5}\ s^{-1}$), the rate of dCTP turnover in Table III ($1.3 \times 10^{-3}\ s^{-1}$), and k_{exo} ($4.5 \times 10^{-3}\ s^{-1}$, Table IV). Since dCMP formation and steady-state 9C/20-mer accumulation occur via partitioning of a common intermediate, k_{5i} is determined from the ratio of rates where dCMP formation/9C/20-mer accumulation = k_{exo}/k_{5i}.

Table VIII: Comparison of Observed and Calculated Kinetic Parameters for dATP Misincorporation into 9/20-mer

	obsd[a]	calcd[b]
k_{cat} (hydrolysis)	5.6×10^{-3} s^{-1}	3.2×10^{-3} s^{-1}
K_M (hydrolysis)	16 μM	10 μM
k_{cat} (misincorporation)	2.1×10^{-3} s^{-1}	2.4×10^{-3} s^{-1}
K_M (misincorporation)	8.3 μM	14.3 μM
k_{exo}	8.2×10^{-3} s^{-1}	9×10^{-3} s^{-1}

[a] The observed values for hydrolysis and misincorporation come from the text and Table II, respectively. k_{exo} is from Table IV. [b] The calculated k_{cat} and K_M values were obtained by computer simulation (see Experimental Procedures) of the model in Scheme V in conjunction with the rate constants in Table VI. Initial velocities of dATP hydrolysis and misincorporation were determined by using the above rate constants at several dATP concentrations. Lineweaver–Burk plots of these data gave the calculated k_{cat} and K_M values.

Hopfield (1980) has proposed that the cleavage of dNTP might be coupled (energy relay) to drive the polymerase into a conformation capable of increased discrimination during the next polymerization cycle. We found, however, identical rates of misincorporation before and after three polymerization cycles (Figure 4), contrary to the predictions of the energy relay model. Similarly, Abbotts and Loeb (1984) found no evidence for an energy relay in eukaryotic pol α and β. However, the energy relay concept has been applied to rationalize an apparent increased 3′→5′-exonuclease discrimination (warm-up) after several polymerization cycles (Papanicolaou et al., 1986; Lecomte & Ninio, 1987).[6] Our data would indicate that for our template–primer, there is no exonuclease warm-up.

Several groups have proposed that cleavage of the incoming dNTP to dNMP and PP_i occurs prior to incorporation (Lecomte et al., 1986; Kunkel et al., 1986; Hopfield, 1974). Support for this idea derived from experiments showing (i) that high levels of PP_i can reduce fidelity (Kunkel et al., 1986), although this is not always observed (Lecomte et al., 1986), and (ii) that [^{32}P]PP_i exchange into incorrect, exogenously added dNMP (Lecomte et al., 1986) occurred during active polymerization. However, we were unable to repeat the [^{32}P]PP_i exchange data.[7] Further, Scheme V can account for PP_i-induced increases and decreases in fidelity through greater competitive inhibition of incorrect (rather than correct) dNTP binding and preferential excision of correctly incorporated dNTPs via pyrophosphorolysis, respectively. Finally, polymerization proceeds with inversion of configuration (Burgers & Eckstein, 1979; Brody & Frey, 1981), whereas prior formation of dNMP should result in retention. We therefore consider it highly unlikely that conversion of the dNTP to dNMP precedes phosphodiester bond formation.

The model in Scheme V can accommodate all of the experimental data and in conjunction with the net rate constants in Table VI accurately predicts the kinetic parameters of dATP misincorporation into 9/20-mer ($^{CG}_{GCAG}$) (Table VIII and Figure 1). Key features on the mechanism include the following: (i) Whereas $K_3 = 100$ for correct polymerization, $K_3 \leq 1$ during dATP misincorporation in order to account for the K_m of dATP. (ii) The pre-steady-state elemental effect requires that the chemical step, k_4, be at least similar to k_3, in contrast to correct polymerization where $k_4 \gg k_3$. (iii) For dATP misincorporation into 9/20-mer, $K_4 \geq 1$, while for dCTP misincorporation into 9/20-mer $K_4 < 1$ to account for the respective presence or absence of a pre-steady-state burst of misincorporation. (iv) The net rate and equilibrium constants for formation of KF′·D_{n+1}·PP_i and k_{exo} largely determine pre-steady-state misincorporation, while k_5 and k_{exo} determine how fast the error accumulates off the enzyme.

The rates of stable misincorporation into DNA varied 10^3-fold (Table I), even among identical misincorporations (G–T), indicating that factors other than just the nature of the mismatch influence misincorporation. This high dependence of pol I catalyzed polymerizations on the neighboring DNA sequence occurs with other DNA sequences (Lai & Beattie, 1988a,b; Fersht et al., 1982; Bryant et al., 1983; Mizrahi et al., 1986; Kuchta et al., 1987) and may be mediated via nearest-neighbor interactions (Randall et al., 1987; Gotoh & Tagashira, 1981; Eritja et al., 1986; Kunkel et al., 1981) as well as sequence-dependent perturbation of the KF·DNA structure. Both 9/20-mer ($^{CCG}_{GGCAGG}$) and 12/36-mer ($^{CCG}_{GGCAGG}$) exhibit similar kinetics of misincorporation; hence, the factors that cause these variable rates are quite localized.

Pol I divides discrimination into three stages. Incorrect dNTPs that are screened out at stage 1 are neither incorporated into DNA nor hydrolyzed to dNMP. Those unable to traverse stage 2 are converted to dNMP but do not accumulate off KF, whereas those edited at stage 3 are stably formed but not locked in by addition of the next correct dNTP and consequently are hydrolyzed to dNMP. Of the misincorporations examined, the majority do not transit stage 2, as exemplified by the 9C/20-mer (Tables I and III). If each stage functioned optimally, the error frequency would be 2.6×10^{-10}, near the maximum estimates for in vivo DNA replication.

The discriminatory mechanism of pol I represents a hybrid of the prescient kinetic proofreading and time delay models of Hopfield (1974) and Ninio (1975), respectively. While this model faithfully describes the kinetic mechanisms by which pol I ensures accurate DNA replication, the precise physical/chemical nature of the steps at which pol I discriminates and the factors that determine how much discrimination each potential error elicits remain obscure. Experiments to elucidate these processes as well as their relationship to the structure of pol I (Joyce & Steitz, 1987) are in progress.

Acknowledgments

We thank Dr. Ken Johnson for helpful discussions and Dwayne Allen and Dr. Carlos Catalano for expert assistance during the DNA synthesis and enzyme purification.

References

Abbotts, J., & Loeb, L. A. (1984) *J. Biol. Chem. 259*, 6712–6714.

Anderson, K. S., Sikorski, J. A., & Johnson, K. A. (1987) *Biochemistry* (submitted for publication).

Barshop, B. A., Wrenn, R. F., & Frieden, C. (1983) *Anal. Biochem. 130*, 134–145.

Bernardi, F., Saghi, M., Dorizzi, M., & Ninio, J. (1979) *J. Mol. Biol. 129*, 93–112.

Boosalis, M. S., Petruska, J., & Goodman, M. F. (1987) *J. Biol. Chem. 262*, 14689–14696.

Brody, R. S., & Frey, P. A. (1981) *Biochemistry 20*, 1245–1252.

Brutlag, D., & Kornberg, A. (1972) *J. Biol. Chem. 247*, 241–248.

[6] Lecomte and Ninio (1987) recently presented evidence in support of an exonuclease warm-up during polymerization by pol I. However, a key assumption for their data analysis is that the rate of polymerization onto a mismatch is identical with the rate onto a correct base pair. The results presented here and by Brutlag and Kornberg (1972) show that this is not true and thus shed doubt on their conclusions.

[7] Lecomte et al. (1986) recently reported the conversion of dTMP and dAMP to [^{32}P]dTTP and [^{32}P]dATP during poly(dC)–oligo(dG) replication in the presence of [^{32}P]PP_i. Under identical conditions we found with either dAMP and poly(dC)–oligo(dG) or dGMP and poly(dA)–oligo(dT) no [^{32}P]dNTP production in the presence of [^{32}P]PP_i.

Bryant, F. R., Johnson, K. A., & Benkovic, S. J. (1983) *Biochemistry 22*, 3537–3546.
Burgers, P. M. J., & Eckstein, F. (1979) *J. Biol. Chem. 254*, 6889–6893.
Clayton, L. K., Goodman, M. F., Branscomb, E. W., & Galas, D. J. (1979) *J. Biol. Chem. 254*, 1902–1912.
Cleland, W. W. (1975) *Biochemistry 14*, 3220.
Cotterill, S. M., Reyland, H. E., Loeb, L. A., & Lehman, I. R. (1987) *Proc. Natl. Acad. Sci. U.S.A. 84*, 5635–5639.
El-Deiry, W., Downey, K. M., & So, A. G. (1984) *Proc. Natl. Acad. Sci. U.S.A. 81*, 7378–7382.
El-Deiry, W., So, A. G., & Downey, K. M. (1988) *Biochemistry 27*, 546–553.
Englisch, V., Gauss, D., Freist, W., Englisch, S., Sternbach, H., & von der Haar, F. (1985) *Angew. Chem., Int. Ed. Engl. 24*, 1015–1025.
Eritja, R., Kaplan, B. E., Mhaskar, D., Sowers, L. C., Petruska, J., & Goodman, M. F. (1986) *Nucleic Acids Res. 14*, 5869–5884.
Ferrin, L. J., Mildvan, A. S. (1986) *Biochemistry 25*, 5131–5145.
Fersht, A. R. (1979) *Proc. Natl. Acad. Sci. U.S.A. 76*, 4946–4950.
Fersht, A. R., Knill-Jones, J. W., & Tsui, W.-C. (1982) *J. Mol. Biol. 156*, 37–51.
Fersht, A. R., Shi, J.-P., & Tsui, W.-C. (1983) *J. Mol. Biol. 165*, 655–667.
Gotoh, O., & Tagashira, Y. (1981) *Biopolymers 20*, 1033–1042.
Gupta, A. P., Benkovic, P. A., & Benkovic, S. J. (1984) *Nucleic Acids Res. 12*, 5897–5911.
Hopfield, J. J. (1974) *Proc. Natl. Acad. Sci. U.S.A. 71*, 4135–4139.
Hopfield, J. J. (1980) *Proc. Natl. Acad. Sci. U.S.A. 77*, 5248–5252.
Joyce, C. M., & Grindley, N. D. F. (1983) *Proc. Natl. Acad. Sci. U.S.A. 80*, 1830–1834.
Joyce, C. M., & Steitz, T. A. (1987) *Trends Biochem. Sci. (Pers. Ed.) 12*, 288–292.
Kornberg, A. (1980) *DNA Replication*, Freeman, San Francisco.
Kuchta, R. D., Mizrahi, V., Benkovic, P. A., Johnson, K. A., & Benkovic, S. J. (1987) *Biochemistry 26*, 8410–8417.
Kunkel, T. A., Schaaper, R. M., Beckman, R. A., & Loeb, L. A. (1981a) *J. Biol. Chem. 256*, 9883–9889.
Kunkel, T. A., Eckstein, F., Mildvan, A. S., Koplitz, R. M., & Loeb, L. A. (1981b) *Proc. Natl. Acad. Sci. U.S.A. 78*, 6734–6738.
Kunkel, T. A., Beckman, R. A., & Loeb, L. A. (1986) *J. Biol. Chem. 261*, 13610–13616.
Lai, M.-D., & Beattie, K. L. (1988) *Biochemistry 27*, 1722–1728.
Lai, M.-D., & Beattie, K. L. (1988) *J. Biol. Chem.* (submitted for publication).
Lecomte, P. J., & Ninio, J. (1987) *FEBS Lett.* (in press).
Lecomte, P., Doubleday, O. P., & Radman, M. (1986) *J. Mol. Biol. 189*, 643–652.
Loeb, L. A., & Kunkel, T. A. (1982) *Annu. Rev. Biochem. 52*, 429–457.
Mizrahi, V., Henrie, R. N., Marlier, J. F., Johnson, K. A., & Benkovic, S. J. (1985) *Biochemistry 24*, 4010–4018.
Mizrahi, V., Benkovic, P., & Benkovic, S. J. (1986) *Proc. Natl. Acad. Sci. U.S.A. 83*, 5769–5773.
Ninio, J. (1975) *Biochimie 57*, 587–595.
Papanicolaou, C., Lecomte, P., & Ninio, J. (1986) *J. Mol. Biol. 189*, 435–448.
Randall, S. K., Entja, R. Kaplan, B. E., Petruska, J., & Goodman, M. F. (1987) *J. Biol. Chem. 262*, 6864–6870.
Setlow, P., Brutlag, P., & Kornberg, A. (1972) *J. Biol. Chem. 247*, 224–231.